ISSN 1063-7788, Physics of Atomic Nuclei, 2022, Vol. 85, No. 6, pp. 528–539. © Pleiades Publishing, Ltd., 2022.
Russian Text © The Author(s), 2022, published in Yadernaya Fizika, 2022, Vol. 85, No. 6, pp. 397–408.

NUCLEI
Experiment

Prospects of Searches for Unstable States in Relativistic Fragmentation of Nuclei

D. A. Artemenkov[1), V. Bradnova[1), O. N. Kashanskaya[2), N. V. Kondratieva[1), N. K. Kornegrutsa[1), E. Mitsova[1),3), N. G. Peresadko[4), V. V. Rusakova[1), R. Stanoeva[5),3), A. A. Zaitsev[1),4)*, I. G. Zarubina[1), and P. I. Zarubin[1),4)

Received June 22, 2022; revised June 22, 2022; accepted June 24, 2022

Abstract—Prospects of the BECQUEREL experiment devoted to studying, within the relativistic approach, problems of nuclear-cluster physics are discussed. The nuclear track emulsion method used in the present study permits fully investigating relativistic final states in the fragmentation of nuclei. The present study focuses on the dynamics of the formation of a ^{8}Be nucleus and the Hoyle state, as well as on searches for the 4α condensate decaying through them. The development of analysis of exposure to ^{84}Kr nuclei at an energy of 950 MeV per nucleon is described in this context. The status of searches for the isobar analog state of the ^{13}N nucleus in the fragmentation of ^{14}N nuclei at an energy of 2 GeV per nucleon is presented as a continuation of studies of light nuclei.

DOI: 10.1134/S1063778822060035

1. INTRODUCTION

The presence of spin-paired proton and neutron quartets in the structure of light nuclei manifests itself in the intense formation of alpha particles in various nuclear reactions and decays [1]. Study of ensembles that consist of several alpha particles permits clarifying the role of ^{8}Be and ^{9}B unstable nuclei and performing searches for their analogs starting from 3α Hoyle state (HS). The alpha-particle clustering is the most pronounced in the ^{8}Be nucleus. The $^8\text{Be} \to 2\alpha$ decay energy is as low as 91.8 keV. The respective decay width, which is 5.57 ± 0.25 eV, corresponds to a lifetime that is eight to nine orders of magnitude longer than the reaction time. The ^{8}Be nucleus inevitably appears among products of ^{9}B and Hoyle state decays. The ground state of the ^{9}B nucleus is higher than the ^{8}Bep threshold by 185.1 keV, and its width, which is 0.54 ± 0.21 keV, also indicates that it is a long-lived state.

The Hoyle state is the second excited state of ^{12}C (for an overview, see [2]) at 378 keV above the 3α threshold. An isolated position of the Hoyle state at the beginning of the ^{12}C excitation spectrum and its width value of $\Gamma(\text{HS}) = 9.3 \pm 0.9$ eV render it a 3α analog of ^{8}Be. The synthesis of ^{12}C in the red-giant medium is possible via the fusion reaction $3\alpha \to \alpha^8\text{Be} \to ^{12}\text{C}(0_2^+) \to ^{12}\text{C}$ ($+2\gamma$ or e^+e^- with a probability of about 10^{-4}). A further synthesis via the fusion reaction $\alpha^{12}\text{C} \to ^{16}\text{O}\gamma$ through a ^{16}O level at an appropriate energy is forbidden in parity. This is the circumstance that determines the relative abundances of ^{12}C and ^{16}O, as well as the survival of ^{12}C under the astrophysical conditions of helium burning. However, the synthesis of ^{16}O is possible through the sequence $^{12}\text{C}^{12}\text{C} \to ^{12}\text{C}^{12}\text{C}(0_2^+) \to ^{16}\text{O}^8\text{Be}$ [2].

Determining the key role of ^{8}Be and of the Hoyle state in nuclear astrophysics, these facts give grounds to assume that the appearance of their heavier analogs is possible. Apart from being an excited state of the ^{12}C nucleus, the Hoyle state may manifest itself in reactions involving other nuclei, and this relates it, in just the same way as ^{8}Be and ^{9}B, to different fragments. Exotically large dimensions predicted theoretically (for example, in [3]) are crucial for obtaining deeper and more general insight into the mechanism of their production and fragmentation. Possessing a structure of nuclear-molecular type, they may serve as source of their own excitation branches and states that have a more complicated composition.

The growth of interest in unstable alpha-particle states was motivated by the concept of an alpha-

[1)]Joint Institute for Nuclear Research , Dubna, Russia.
[2)]Francisk Skorina Gomel State University , Gomel, Belarus.
[3)]Institute for Nuclear Research and Nuclear Energy, Bulgarian Academy of Sciences, Sofia, Bulgaria.
[4)]Lebedev Physical Institute of the Russian Academy of Sciences, Moscow, Russia.
[5)]Southwest University Neofit Rilski, Blagoevgrad, Bulgaria.
*E-mail: zaicev@jinr.ru

particle Bose–Einstein condensate (αBEC). This concept was put forth in the early 2000s by analogy with quantum gases in atomic physics (for an overview, see [3]). The excitations of $n\alpha$-tuple nuclei immediately above the alpha-particle binding energies may serve as αBEC manifestations. Coexisting with fermion excitations, they are treated on the basis of a boson mean field formed by a gas of nearly ideal bosons in the S state at an average density one-fourth as large as an ordinary density. The ^{8}Be nucleus and Hoyle state are described as 2- and 3αBEC states, and their decays may be viewed as signatures of more complicated decays of $n\alpha$BEC states. The existence of heavier analogs of the Hoyle state may enrich scenarios of nucleosynthesis toward heavy nuclei. The experimental approaches proposed with aim of searches for αBEC in the fragmentation of light nuclei include that described in the present article below (for overview, see [4]). We focus on the 0_6^+ state of the ^{16}O nucleus at 15.1 MeV (660 keV above 4α threshold), considering it as a state that is a 4α analog of the Hoyle state and which decays to α and the Hoyle state or to 2^{8}Be. The treatment of $n\alpha$BEC as loosely bound unstable states opens new possibilities for their searches as the energy and mass numbers of progenitor nuclei grow. It would be of value to demonstrate the universality of $n\alpha$BEC candidates on the basis of relativistic invariance.

In the fragmentation of relativistic nuclei, the ensembles of helium nuclei and protons are produced within a very narrow cone. There are no detection thresholds for them, and the energy losses are minimal. Because of an extremely low energy, ^{8}Be, ^{9}B, and Hoyle state decays should manifest themselves as pairs and triples of He and H relativistic fragments with the smallest opening angles. The width values suggest that ^{8}Be, ^{9}B and Hoyle state decays occur at ranges between several thousand (^{8}Be and HS) and several tens of (^{9}B) atomic radii and that their identification should rely on the criterion of a minimum invariant mass. An answer to these challenges is provided by the nuclear-emulsion method, whose application is being continued in the BECQUEREL experiment. In nuclear-emulsion layers exposed longitudinally to relativistic nuclei, the fragment tracks are observed completely, whereas their directions are measured with the highest resolution. The determination of invariant masses of ensembles of He and H relativistic fragments in the approximation of conservation the velocity of the parent nucleus make it possible to project their angular correlations onto the relative energy scale starting from ^{8}Be decay. The potential and status of these investigations are surveyed in [5–7]. The identification of ^{8}Be, ^{9}B, and the Hoyle state in the fragmentation of light nuclei, including radioactive ones [6], are among the achievements reached along these lines.

In the BECQUEREL experiment, it was proposed to extend this approach to searches for αBEC states in events of fragmentation of medium mass and heavy nuclei. A fast growth of the ^{8}Be, ^{9}B, and Hoyle state contributions with increasing number of accompanying alpha particles was discovered recently. This effect may be explained within the picture that combines the production of alpha particles with the growth of their density in the phase space [7]. This scenario gives grounds to assume that αBEC arises owing to the formation of states belonging to the αBEC type via a sequential pickup of accompanying alpha particles rather than owing to an appropriate excitation of the parent nucleus. In this case, αBEC may be viewed as a short-lived state that arises in nuclear matter of extremely low density and temperature and which has nothing to do with the excitation of the parent nucleus. The selection of events characterized by a high multiplicity of alpha particles may be used as an enhancing factor in the statistics of events that are αBEC candidates. Thus, αBEC searches based on the invariant mass of ensembles of relativistic alpha particles that have extremely close 4-momenta are the nearest objective pursued by the BECQUEREL experiment and discussed below.

At the same time, investigation of unstable state formation by light nuclei will be continued in what is concerned with searches for isobar analog states by the nuclear track emulsion (NTE) method in the relativistic implementation. Because of mass effects, this would correspond to a substantially higher energies and, at the same time, to rather small widths. The available irradiations of nuclear track emulsions with ^{14}N, ^{22}Ne, ^{24}Mg, and ^{28}Si relativistic nuclei are worthy of analysis in this context. Searches for ^{13}N(15.065), ^{8}Be(16.6 + 16.9), and ^{9}B(14.7) isobar analog states in the fragmentation processes $^{14}\mathrm{N} \to 3\alpha p$, $^9\mathrm{Be} \to 2\alpha$, and $^{10}\mathrm{C} \to 2\alpha 2p$, respectively, are currently under way. Preliminary results of these searches will be presented below.

2. POTENTIAL OF THE NUCLEAR-EMULSION METHOD

Possibilities provided by the NTE method, which remain unique within the realms being discussed, are worth recalling. Exposed stacks are assembled from layers that have an area of up 10×20 cm^2 and a NTE thickness of 200 μm on a glass substrate and 550 μm without it. If the beam axis is parallel to the emulsion-layer plane, then the tracks of all relativistic fragments remain sufficiently long within one layer for a three-dimensional reconstruction of angles to be implemented. The substrate ensures the “stiffness” of tracks, and its absence permits introducing them in neighboring layers. The emulsion thickness and a full solid angle of detection are factors that contribute to collecting vast statistics. Nuclear emulsions contain, in close concentrations, atoms of Ag and Br and atoms of the CNO group, as well as hydrogen atoms whose concentration is three times higher. Via scanning, under microscopes with a 20-fold amplification, the tracks of the nuclei being studied, one can observe about one thousand interactions not subjected any selection or several tens of peripheral interactions. A sample of several hundred peripheral interactions characterized by specific configurations of relativistic fragments can be obtained in the case of transverse scanning.

Tracks of He and H relativistic fragments identified visually according to their charge are concentrated within a cone bounded by $\sin\theta_{\rm fr} = p_{\rm fr}/P_0$, where $p_{\rm fr} = 0.2$ GeV/c characterizes the Fermi momentum of nucleons in the projectile nucleus and P_0 is the projectile momentum per nucleon. Owing to granularity of about 0.5 μm, the angular resolution over a base of 1 mm is not poorer than 10^{-3} rad. The transverse momentum P_T of a fragment with mass number $A_{\rm fr}$ is given by $P_T \approx A_{\rm fr} P_0 \sin\theta$ in the approximation of P_0 conservation. The assignment of the H and He mass numbers is possible on the basis of measurements of average multiple scattering angles. The use of this cumbersome procedure is advisable in particular cases for a limited number of tracks. In the case of dissociation of stable nuclei, it is sufficient to assume the He—^{4}He and H—^{1}H correspondence. This simplification is even more justified in the case of extremely narrow decays of ^{8}Be and ^{9}B [6].

The tracks of b particles (alpha particles and protons of energy below 26 MeV), g particles (protons of energy above 26 MeV), and s particles (product mesons) may be observed in the fragmentation of NTE nuclei. The fact that fragments retain the charge of beam nuclei in an event where the number of slow fragments is moderately small is used as a criterion of selection of peripheral interactions, which constitute several percent of the total number of stars. The most peripheral interactions, which are called coherent dissociations or white stars, are not accompanied by the the fragmentation of target nuclei or by meson production. For photographs and videos of characteristic interactions, we refer the interested reader to the http://becquerel.jinr.ru/ website.

The invariant mass of an ensemble of relativistic fragments is determined as the sum of the products of the fragment 4-momenta $P_{i,k}$, $M^{*2} = \sum(P_i P_k)$. The subtraction of the mass of the primary nucleus or the sum of the fragment masses, $Q = M^* - M$, is the issue of convenience of representation. The components $P_{i,k}$ are determined in the approximation of P_0 conservation for the fragments. The reconstruction implemented in the BECQUEREL experiment on the basis of the invariant mass in the decays of ^{8}Be and ^{9}B relativistic unstable nuclei confirmed the validity of this approximation [6].

The highest precision of the measurements is ensured upon the application of the coordinate method with KSM-1 microscopes (Carl Zeiss, Jena) with 60-fold magnification in immersion oil. The measurements are performed in a Cartesian system of coordinates. The NTE layer is rotated in such a way that the direction of the primary track under analysis complies with the OX axis of the microscope table within a deviation of 0.1 to 0.2 μm per 1 mm of length. The OX axis of the coordinate system then complies with the direction of the primary track projection onto the layer plane, while the OY on it is orthogonal to the primary track. The OZ axis is orthogonal to the layer plane. The measurements are performed by means of the horizontal-translation microscrews along the OX and OY axes and by means of the sharpness-depth microscrew along the OZ axis. The coordinates are measured along primary and secondary tracks over lengths of 1 to 4 mm with a step of 100 μm. The planar and immersion angles are calculated on the basis of their linear approximation.

3. STATUS OF THE INVESTIGATIONS

Searches for αBEC are predominantly based on the use of compact spectrometers providing a large solid-angle acceptance and are performed in experiments with beams of light nuclei at energies of several tens of MeV units per nucleon [5, 8—13]. Silicon detectors characterized by the highest energy resolution and positioned within vacuum volumes near ultrathin targets are employed for this. Unstable nuclei and states are identified on the basis of angular and energy correlations in detected ensembles of alpha particles.

The experiment reported in [8] and implemented in such a way that it permitted a complete detection of alpha-particle projectile fragments in the ^{40}Ca(25 MeV/nucleon) + ^{12}C reaction showed a growing contribution of ^{8}Be up to the alpha-particle multiplicity of six. This contradicts the model that predicts its reduction (see Table 2 in [8]). Searches for decays of the ^{16}O(0^+_6, 15.1 MeV) state in the ^{20}Ne(12 MeV/nucleon + ^{4}He) and ^{16}O(160, 280, 400 MeV) + ^{12}C reactions were performed in [9] and [11], respectively. Data obtained for the reaction ^{16}O(45 MeV)$+^{12}C \to 4\alpha$ in a complete kinematics [13] were recently analyzed for all possible configurations. The excitation function was reconstructed directly for the 4α channel, as well as for particular reaction channels, such as $^{12}C(0_2^+)\alpha$, $^{12}C(3_1^-)\alpha$, and 2^8Be. However, searches for the 15.1-MeV state did not lead to a positive result in all of the cases [12]. Measurements of coincidences of alpha particles (at 386 MeV) scattered at zero angle in the reaction $^{20}Ne(\alpha,\alpha')5\alpha$ were performed [5]. It is stated that the newly observed states at 23.6, 21.8, and 21.2 MeV in ^{20}Ne are intimately related to the ^{16}O 4αBEC candidate and may be viewed themselves as candidates for αBEC.

Although the status of observations of αBEC remains uncertain [11], it turns out that, in all cases, the Hoyle state arises from the fragmentation of not only ^{12}C. This circumstance is indicative of the progenitor independence of both the Hoyle state and the ^8Be nucleus. Candidates for αBEC are also expected to exhibit universality of this kind. By and large, it seems that, in what concerns statistics, experiments aimed at searches for 4αBEC states approached a limit accessible in practice. It is necessary to address peripheral collisions of heavier nuclei that would have higher energies. In order to unify data obtained in the widest possible energy range and to confirm, on this basis, the universality of αBEC, it is required to represent unstable states in a relativistically invariant form.

Electron experiments in beams of relativistic nuclei did not overcome difficulties associated with the quadratic dependence of ionization on charges, an extremely small divergence of relativistic fragments and beam nuclei, and their coincidence in the magnetic rigidity. An object-oriented application of the NTE method, which is technically straightforward and is not expensive, is the only practicable alternative. This method provides flexibility and consistency at the stage of searches and clarity of interpretation in the theoretical aspect. Exposures of NTE stacks to light nuclei of energy equal to several GeV units per nucleon at the synchrophasotron of Joint Institute for Nuclear Research (JINR, Dubna) and at LBL's Bevalac (Betatron) started in the 1970s, while exposures to medium-mass and heavy nuclei at substantially higher energies began in the 1990s at Alternating Gradient Synchrotron (AGS, Brookhaven National Laboratory) and Super Proton Synchrotron (SPS, CERN). The results of these irradiations and NTE layers were preserved in the BECQUEREL experiment. They form a data set that is unique at the present time in what concerns relativistic fragmentation and which includes, among other things, identification of ^8Be. The latter proves observation of final states down to the minimum decay energy. By and large, this fact served as a motivation for choosing nuclear clustering as an object of study by the NTE method in the relativistic approach.

Since the early 2000s, the application of the NTE method has been continued in the BECQUEREL experiment at the JINR Nuclotron with the aim of studying the fragmentation of light nuclei (for an overview, see [5, 6]). Special features of the isotopes $^{7,9}Be$, $^{8,10,11}B$, $^{10,11}C$, and $^{12,14}N$ manifested themselves in the probabilities for dissociation channels. The decay processes $^9B \to {}^8Be\,p$ were identified on the basis of the invariant mass calculated under the assumption of primary momentum conservation. It was shown that the NTE resolution was a necessary and sufficient condition. The selection of ^8Be was determined by a cut at 0.2 MeV (see Figs. 1*a* and 1*b*), while the selection of ^9B was determined by a cut at 0.5 MeV (see Fig. 1*c*).

The identification of ^8Be and ^9B nuclei became a motivation to perform searches for Hoyle state decays in the dissociation process $^{12}C \to 3\alpha$ (see Fig. 1*d*), where a cut of 0.7 MeV was set on the 3α invariant mass. The choice of these three conditions as upper bounds is sufficient since the values of the decay energy for these three states are substantially lower than the closest excitations that have the same nucleon composition and since the reflection of more complex excitations is not significant for these nuclei.

An analysis of $^{12}C \to 3\alpha$ and $^{16}O \to 4\alpha$ white stars not accompanied by target fragments made it possible to prove that the fraction of events containing ^8Be (Hoyle state) decays is $45 \pm 4\%$ ($11 \pm 3\%$) for ^{12}C and $62 \pm 3\%$ ($22 \pm 2\%$) for ^{16}O (see Fig, 1*b*). One can see that an increase in the number of 2α and 3α combinations enhances the contribution of ^8Be and the Hoyle state. This observation calls for a verification for heavier nuclei, in which case the combinatorics of alpha particles grows sharply with mass number.

A simple selection of the above decays became possible owing to the fact that the values of the decay energy for these three states are substantially lower than the closest excitations that have the same nucleon composition, the reflection of more complex excitations being insignificant. The same approach can be extended to further searches for states immediately above the alpha-particle binding energies. The possible formation of the Hoyle state through the alpha decay of $^{16}O(0_6^+)$ was explored. The distribution of $^{16}O \to 4\alpha$ white stars with respect to the 4α invariant mass $Q_{4\alpha}$ (see Fig. 2) is described, for the most part, by a Rayleigh distribution with parameter $\sigma Q_{4\alpha} = (6.1 \pm 0.2)$ MeV. The condition $Q_{3\alpha}(\mathrm{HS}) < 700$ keV shifts the $Q_{4\alpha}$ distribution toward lower energies. A magnified shape of the $Q_{4\alpha}$ distribution (see inset in Fig. 2*a*) is indicative of the presence of nine events

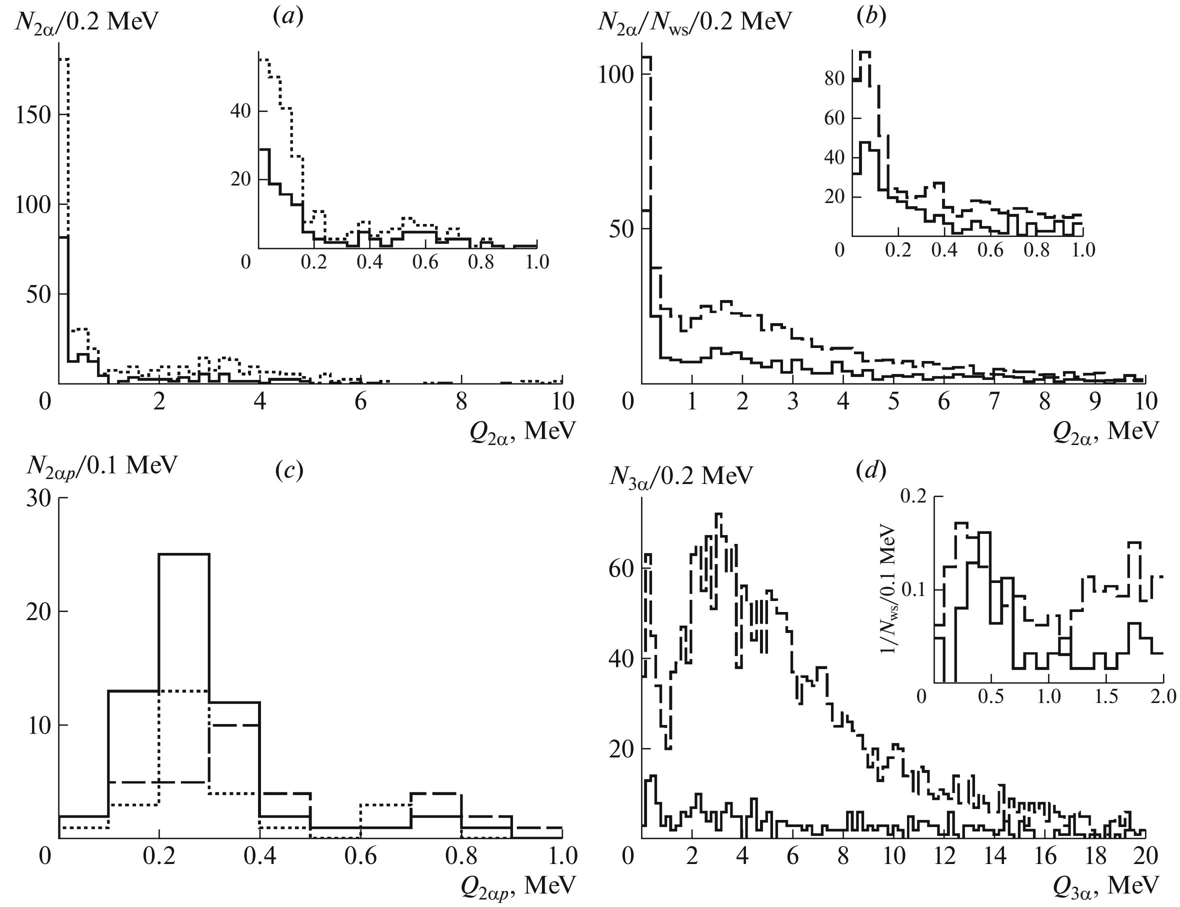

Fig. 1. Invariant-mass distributions [7]: (*a*) $Q_{2\alpha}$ in ^{9}Be(1.2 GeV/nucleon) $\to 2\alpha$ (dotted curve) and white stars (solid curve); (*b*) $Q_{2\alpha}$ in ^{12}C(3.65 GeV/nucleon) $\to 3\alpha$ (solid curve) and ^{16}O(3.65 GeV/nucleon) $\to 4\alpha$ (dashed curve); (*c*) $Q_{2\alpha p}$ (<1 MeV) in ^{10}C(1.2 GeV/nucleon) $\to 2\alpha 2p$ (solid curve), ^{11}C(1.2 GeV/nucleon) $\to 2\alpha 2p$ (dotted curve), and ^{10}B(1 GeV/nucleon) $\to 2\alpha p$ (dashed curve); and (*d*) $Q_{3\alpha}$ in ^{12}C(3.65 GeV/nucleon) $\to 3\alpha$ (solid curve) and ^{16}O(3.65 GeV/nucleon) $\to 4\alpha$ (dashed curve).

that satisfy the condition $Q_{4\alpha} < 1$ MeV and for which the mean value is $\langle Q_{4\alpha}\rangle(\mathrm{RMS}) = 624 \pm 84(252)$ keV. The contribution of the decay processes $^{16}\mathrm{O}(0_6^+) \to \alpha + \mathrm{HS}$ is then estimated at $1.4 \pm 0.5\%$ in the case of normalization to $N_{\mathrm{ws}}(^{16}\mathrm{O})$ and at $7 \pm 2\%$ in the case of normalization to $N_{\mathrm{HS}}(^{16}\mathrm{O})$.

Thirty-three $^{16}\mathrm{O} \to 2^8\mathrm{Be}$ events were identified. This value constitutes $5 \pm 1\%$ of $^{16}\mathrm{O} \to 4\alpha$ white stars. The ratio of events in the $^{16}\mathrm{O} \to 2^8\mathrm{Be}$ and $^{16}\mathrm{O} \to \alpha\mathrm{HS}$ data samples is then 0.22 ± 0.02. The distribution of $^{16}\mathrm{O} \to 2^8\mathrm{Be}$ events with respect to the invariant mass $Q_{4\alpha}$ in Fig. 2*b* is indicative of the presence of two $^{16}\mathrm{O}(0_6^+) \to 2^8\mathrm{Be}$ candidates in the region of $Q < 1.0$ MeV. Thus, the estimated ratio of the probabilities for the channels $^{16}\mathrm{O}(0_6^+) \to 2^8\mathrm{Be}$ and $^{16}\mathrm{O}(0_6^+) \to \alpha\mathrm{HS}$ is 0.22 ± 0.17. We can conclude that, although direct dissociation is dominant in Hoyle state production, the search for its 4α precursor is possible. Since the enlargement of statistics of $^{16}\mathrm{O} \to 4\alpha$ events was exhausted, investigation of alpha-particle ensembles was continued for heavier nuclei.

4. UNSTABLE STATES IN THE DISSOCIATION OF KRYPTON NUCLEI

It is hardly probable that the states considered above form a universal, albeit exotic, part of the structure of nuclei studied thus far. The formation of ^{8}Be nuclei in the interaction of pairs of alpha particles already produced is an alternative possibility. This may be followed by the pickup of other alpha particles and nucleons by ^{8}Be nuclei. As the alpha-particle multiplicity $n\alpha$ becomes higher, it is natural to expect the growth of the ^{8}Be yield and, possibly, of the ^{9}B and Hoyle state yields. Within this scenario, $n\alpha$BEC states can be sequentially produced. On the contrary, one could expect an inverse correlation within the first scenario—the growth of $n\alpha$ would lead to a deficit of ^{8}Be.

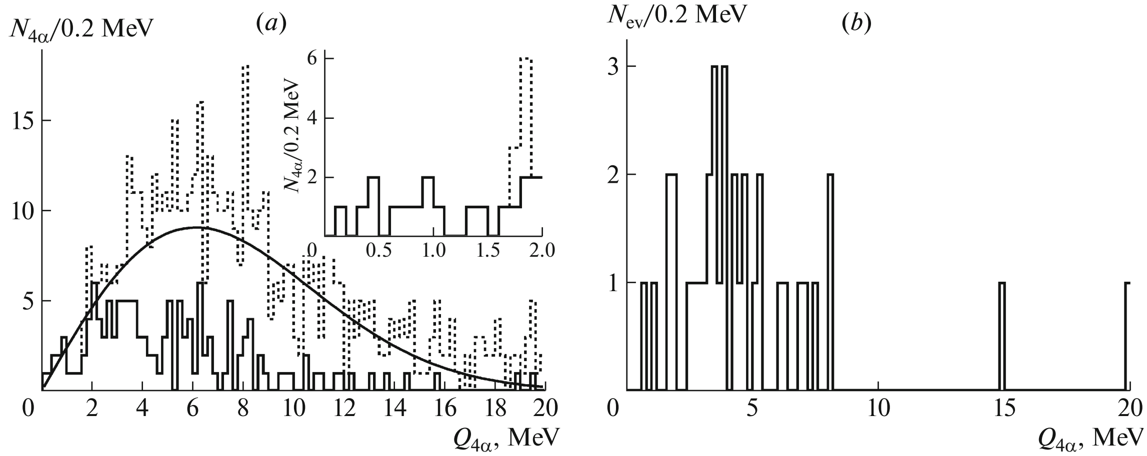

Fig. 2. Distribution of the invariant mass $Q_{4\alpha}$ [7] in 641 $^{16}O \to 4\alpha$ white stars at 3.65 GeV per nucleon for all 4α configurations (a, dotted line), αHS events (a, solid line), and $^{16}O \to 2^8Be$ events (b). The smooth curve represents a Rayleigh distribution. The magnified part for $Q_{3\alpha} < 2$ MeV is given in the inset.

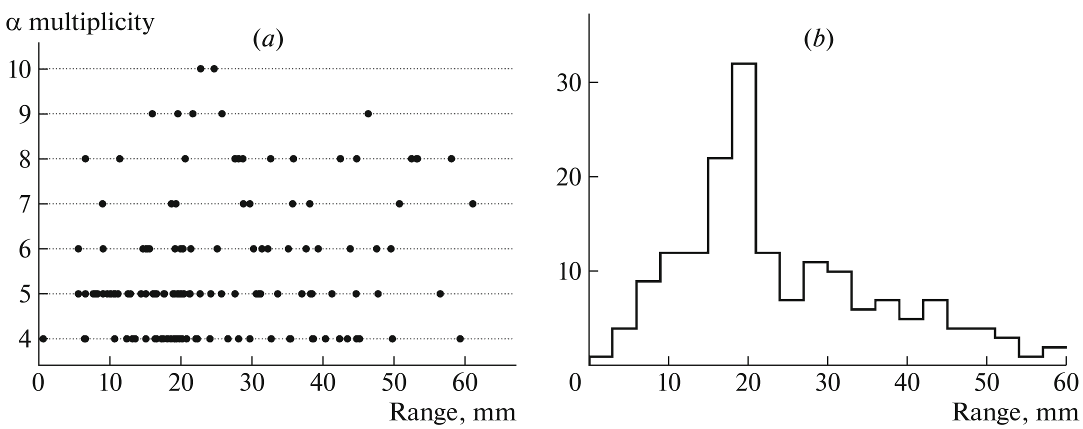

Fig. 3. (a) Multiplicity distribution of product alpha particles versus the longitudinal coordinate of the interaction vertex; (b) distribution of events with respect to the range of krypton nuclei to the interaction vertex.

The results of the emulsion collaboration that were obtained by measuring the interactions of ^{16}O, ^{22}Ne, ^{28}Si, and ^{197}Au nuclei at the JINR synchrophasotron and the results obtained by the EMU Collaboration at AGS [14] by scanning along tracks (that is, without selections) were analyzed in this context. A wide coverage in $n\alpha$ permitted measuring 1316 inelastic interactions of ^{197}Au at 10.7 GeV/nucleon, and the fraction of $n\alpha > 3$ events among them turned out to be 16%. Since a complication of the measurements in question was needed, the more lenient selection criterion of $Q_{2\alpha}(^8Be) \leqslant 0.4$ MeV was imposed. It turned out that the ratio of the number $N_{n\alpha}(^8Be)$ of events featuring at least one identified ^8Be decay to $N_{n\alpha}$ exhibits a strong growth with increasing $n\alpha$.

The interactions of ^{197}Au involves triples subjected to the selection criteria of $Q_{2\alpha p}(^9B) \leqslant 0.5$ MeV and $Q_{3\alpha}(HS) \leqslant 0.7$ MeV. The ratios of the event numbers $N_{n\alpha}(^9B)$, $N_{n\alpha}(HS)$, and $N_{n\alpha}(2^8Be)$ to $N_{n\alpha}(^8Be)$ do not show a sizable change with $n\alpha$, suggesting a growth with respect to $N_{n\alpha}$. However, only this trend can be noticed because of the scantiness of statistics. Summation of $N_{n\alpha}(^9B)$, $N_{n\alpha}(HS)$, and $N_{n\alpha}(2^8Be)$ over the multiplicities of $n\alpha$ and a normalization to the sum of $N_{n\alpha}(^8Be)$ lead to the relative contributions of $25 \pm 4\%$, $6 \pm 2\%$, and $10 \pm 2\%$, respectively. The distribution of $Q_{4\alpha}$ indicates that alpha-particle quartets (4α) appear nearly at the very threshold and permits the reconstruction of Hoyle state and 2^8Be decays among them upon imposing the condition $Q_{2\alpha}(^8Be) \leqslant 0.2$ MeV. Of these decays, one, for which $Q_{4\alpha} = 1.0$ (16α, HS) MeV provides a guideline for 4αBEC searches.

At the present time, the statistics of $n\alpha$ ensembles is being extended via a transverse scanning of NTE layers irradiated with ^{84}Kr nuclei at 950 MeV per nucleon (GSI, early 1990s) [15]. The distributions of $n\alpha$ and the longitudinal coordinates of interaction vertices for events that were found are shown in Fig. 3. In this case, the energy loss is approximately uniform up to 6 cm and amounts to about 9 MeV/mm (the total range is about 8 cm) [16]. This effect is taken into account on the basis of the range to each interaction vertex via respectively reducing the alpha-particle momentum in calculating $Q_{(2-4)\alpha}$. Moreover, the fragment momentum is taken with a coefficient of 0.8. This coefficient, which is immaterial for the selection criterion $Q_{2\alpha}(^{8}\mathrm{Be}) \leqslant 0.4$ MeV, permits, in the following, retaining the selection condition $Q_{3\alpha}(\mathrm{HS}) < 0.7$ MeV with an eye to the $Q_{3\alpha}(\mathrm{HS})$ peak.

Figure 4*a* shows the $Q_{2\alpha}$ distribution of 173 measured stars for which $n\alpha > 3$. In order to reach the best selection of ^{8}Be decays, the emission angles were determined in this data sample on the basis of values averaged over five-fold measurements of coordinates of five points along the track of each alpha particle at a distance of up to 500 μm from the interaction vertex. This distribution was supplemented with the $Q_{2\alpha}$ values for 184 $n\alpha > 3$ stars from the total number $N_{\mathrm{ev}} = 875$ of interactions of ^{84}Kr nuclei at energies ranging from 950 down to 800 MeV per nucleon [15]. For want of information about the positions of the vertices, the energy was set to 875 MeV per nucleon, while the coefficient of 0.8 was not used. This choice was not critical for identification on the basis of the selection criterion $Q_{2\alpha}(^{8}\mathrm{Be}) \leqslant 0.4$ MeV. Figure 4*b* shows distributions of tracks of alpha particles under the condition of $Q_{2\alpha}(^{8}\mathrm{Be}) \leqslant 0.4$ MeV in polar angles with respect to the direction of tracks of krypton nuclei.

The statistics $N_{n\alpha}$ of $n\alpha > 3$ stars in the new measurements and in the data in [15] are close. The similarity of the distributions of $N_{n\alpha}$ with respect to $n\alpha$ within the statistical uncertainties is indicative of the correctness of transverse scanning. The ratio $N_{n\alpha}/N_{\mathrm{ev}}$ based on the data reported in [15] gives an idea of the contribution of $n\alpha > 3$ stars to the cross section for interaction with emulsion nuclei. Table 1 gives statistics of $n\alpha > 3$ stars that feature at least one or two decays of ^{8}Be, as well as the Hoyle state. The statistics of both samples are summed in the ratio $N_{n\alpha}(\geqslant 1\,^{8}\mathrm{Be})/N_{n\alpha}$. We can conclude that the universal effect of an increase in the probability for finding ^{8}Be in an event as $n\alpha$ grows in this event manifests itself for yet another nucleus and at the lowest energy value.

The new measurements made it possible to identify 12 decays of $2\,^{8}$Be and nine decays of the Hoyle state (see Table 1). The distribution of $Q_{3\alpha}$ up to 2 MeV in Fig. 5*a* shows the expected concentration of alpha-particle triples in the vicinity of the Hoyle state decay energy. Adopting this fact as a calibration, we also introduce the coefficient of 0.8 for the alpha-particle momenta in the calculation of $Q_{4\alpha}$. Figure 5*b* shows the distributions of alpha-particle tracks for $Q_{3\alpha}(\mathrm{HS}) \leqslant 0.4$ MeV in polar angles with respect to the direction of tracks of krypton nuclei.

The distributions of $Q_{4\alpha}$ up to 10 MeV are presented in Fig. 6 under the conditions $Q_{2\alpha}(^{8}Be) \leqslant 0.4$ MeV and $Q_{3\alpha}(\mathrm{HS}) < 0.7$ MeV (*a*) and under the condition $Q_{2\alpha}(^{8}Be) \leqslant 0.4$ MeV imposed on two alpha-particle pairs (*b*). Either of these two distributions suggest the presence of a 4α quartet at $n\alpha = 6$ with an isolated value of $Q_{4\alpha} = 0.6$ MeV corresponding both to the αHS version and to the $2\,^{8}$Be version. With allowance for a correction in this event, the energy of the krypton nucleus is 700 MeV per nucleon, while the polar angles in the alpha-particle quartet with respect to the direction of the traces of krypton nuclei are 58, 63, 73, and 75×10^{-3} rad. Without contradicting $^{16}\mathrm{O}(0_6^+)$ decay, this single observation serves as a starting point for a further accumulation of statistics concerning the 4αBEC problem.

5. ISOBAR ANALOG STATES IN LIGHT NUCLEI

Study of unstable states indicates that searches for more complex states in light nuclei are possible: we mean here isobar analog states suggesting rearrangement toward similarity to less stable isotopes characterized by a less degree of alpha-particle clustering. Although isobar analog states lie at rather high energies (13 to 18 MeV), they have widths Γ that are smaller than those of neighboring excitations because of the $\Delta T = 1$ isospin forbiddenness of their decays—that is, a higher degree of alpha-particle clustering. It can be assumed that, in light nuclei, $T = 1$ *hn* and *tp* configurations are excited in isobar analog states up to the binding energy (see Fig. 7). Here, a ^{3}He cluster is denoted by h (helion). This virtual transition may be due to a nucleon spin flip in the alpha-particle quartets *nn*–*pp* (see Fig. 7*a*). It is impossible in a free alpha particle but may manifest itself in the diffraction scattering of alpha particles.

A manifestation of *hn*–*tp* pairs can be traced starting from ^{8}Be (see Fig. 7*b*), where there is a doublet of isospin-mixed $(T = 0 + 1)$ excitations $^{8}\mathrm{Be}(16.6)$, whose width is $\Gamma = 108$ keV, and $^{8}\mathrm{Be}(16.9)$, whose width is $\Gamma = 74$ keV. Lying below the $^{7}\mathrm{Li} + p$ threshold (17.255) and decaying to an alpha-particle pair exclusively, these levels are candidates for the $\alpha + (hn/tp)$ configuration. The $^{8}\mathrm{Be}(16.6 + 16.9)$ levels lie rather far from the closest excitation $^{8}\mathrm{Be}_{4+}(11.4)$ of

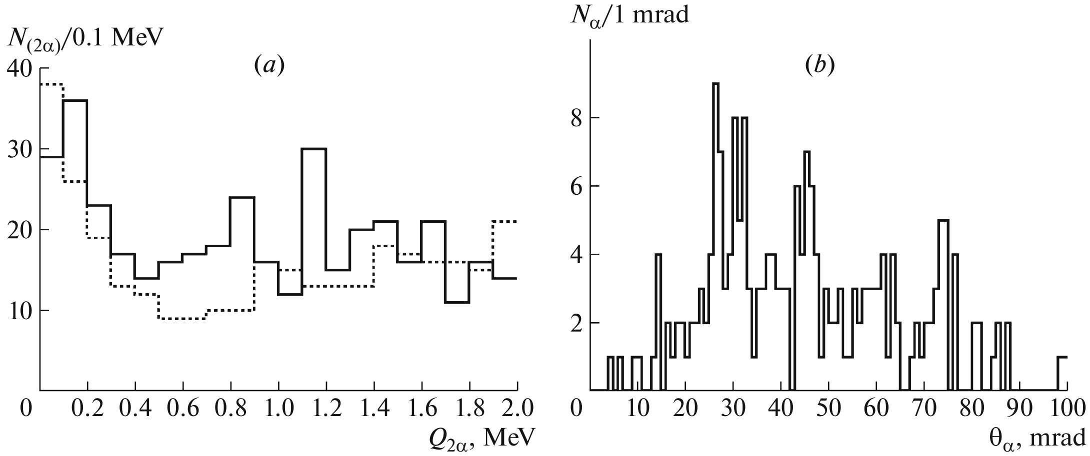

Fig. 4. Distribution of all combinations of pairs of alpha particles produced in the fragmentation of ^{84}Kr nuclei with respect to the invariant mass $Q_{2\alpha} < 2$ MeV (a) according to new measurements and data obtained earlier [15] (dotted curve) and distribution of tracks of alpha particles subjected to the condition $Q_{2\alpha}(^8\mathrm{Be}) \leqslant 0.4$ MeV with respect to polar angles (b).

Table 1. Statistics $N_{n\alpha}$ of $n\alpha > 3$ stars (statistics of the data sample from [14] is given in parentheses)

$n\alpha$	4	5	6	7	8	9–13
$N_{n\alpha}$	40(69)	50(54)	21(27)	10(19)	15(12)	7(3)
$N_{n\alpha}/N_{\mathrm{ev}}$, %	(7.9 ± 1.0)	(6.2 ± 0.9)	(3.1 ± 0.6)	(2.2 ± 0.5)	(1.4 ± 0.4)	(0.4 ± 0.2)
$N_{n\alpha}(\geqslant 1^8\mathrm{Be})$	5(15)	16(10)	12(13)	4(10)	11(8)	4(3)
$N_{n\alpha}(\geqslant 1^8\mathrm{Be})/N_{n\alpha}$, %	19 ± 5	25 ± 6	52 ± 13	48 ± 16	70 ± 21	70 ± 35
$N_{n\alpha}(2^8\mathrm{Be})$	0	2	2	1	5	2
$N_{n\alpha}(\mathrm{HS})$	1	2	1	1	2	2

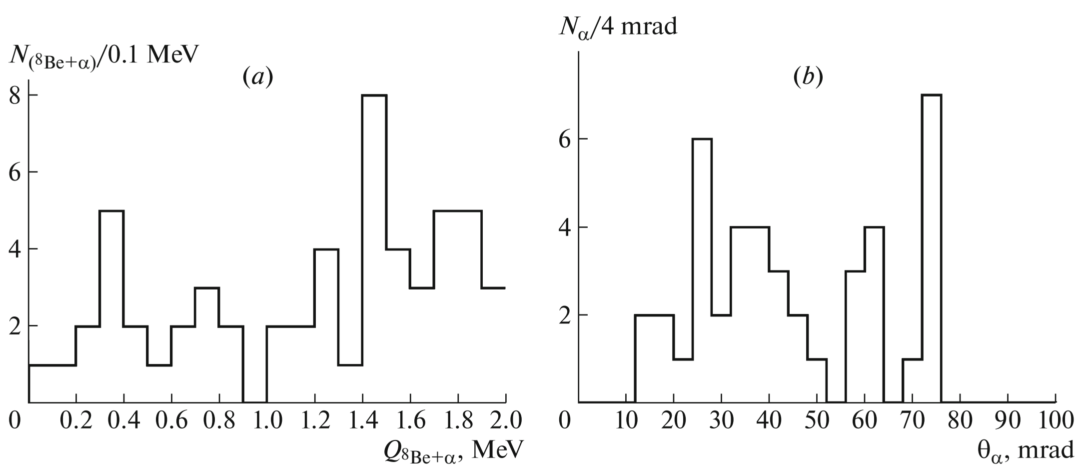

Fig. 5. (a) Distribution of all combinations of triples of alpha particles in the region of $Q_3\alpha < 2$ MeV under the condition $Q_2\alpha(^8\mathrm{Be}) \leqslant 0.4$ MeV imposed on the invariant mass that were produced in the fragmentation of ^{84}Kr nuclei and (b) distributions of tracks of alpha particles for $Q_3\alpha(\mathrm{HS}) \leqslant 0.7$ MeV with respect to polar angles in the region of $Q_2\alpha(^8\mathrm{Be}) \leqslant$ 0.4 MeV.

width $\Gamma = 3.5$ MeV, and this permits their simultaneous identification in the relativistic-fragmentation process $^9\mathrm{Be} \to 2\alpha$. Higher them they, there is the $T = 1$ isobar analog state ^{8}Be(17.640) of width $\Gamma =$

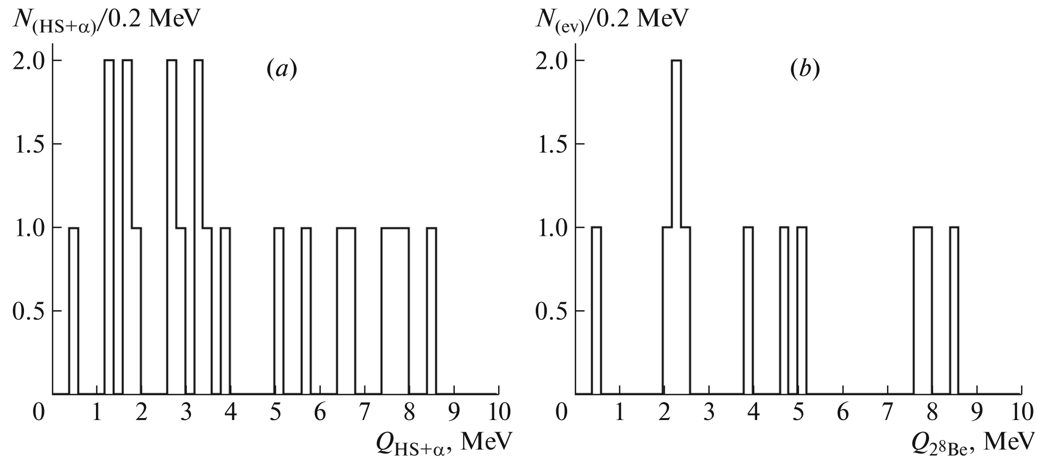

Fig. 6. Invariant-mass distribution of all combinations of alpha-particle quartets from the fragmentation of ^{84}Kr nuclei in the region of $Q_{3\alpha} < 10$ MeV under the conditions of $Q_{2\alpha}(^8\mathrm{Be}) \leqslant 0.4$ MeV and $Q_{3\alpha}(\mathrm{HS}) < 0.7$ MeV (a) (a) and under the condition of $Q_{2\alpha}(^8\mathrm{Be}) \leqslant 0.4$ MeV imposed on two alpha-particle pairs (b).

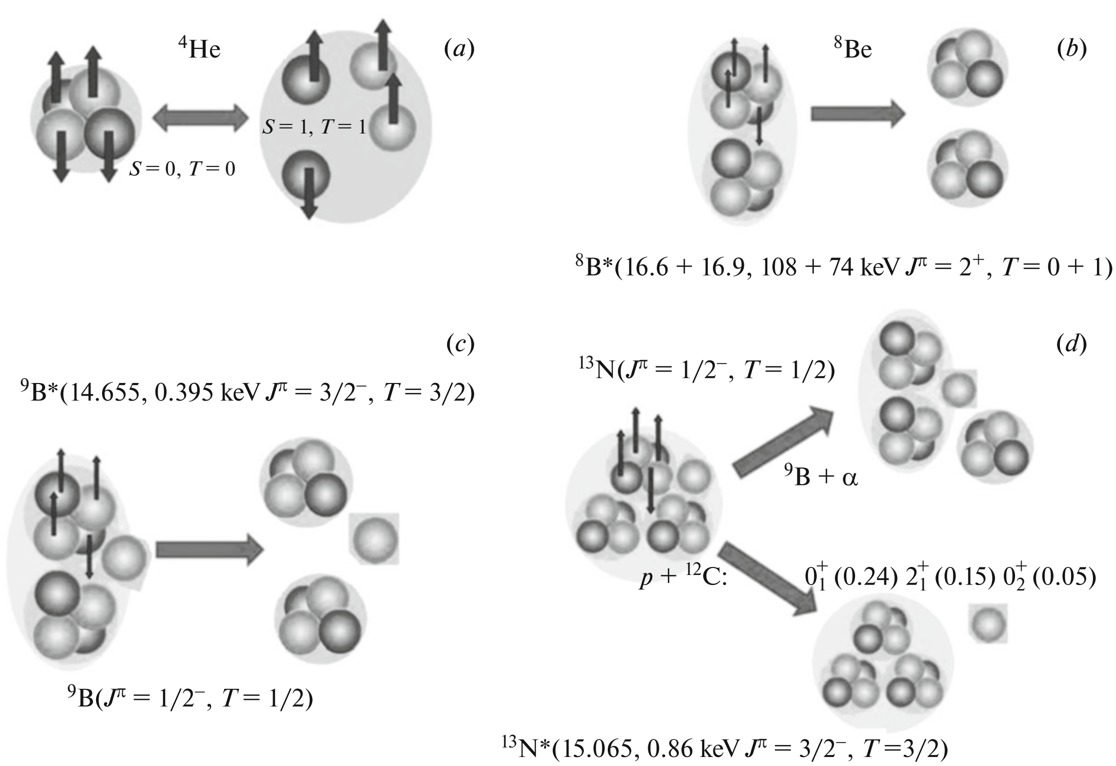

Fig. 7. Scenario of the emergence of an isobar analog state owing to the excitation of an alpha-particle configuration in (a) light nuclei, (b) ^{8}Be, (c) ^{9}B, and (d) ^{13}N.

10.7 keV above the threshold for isospin-allowed decay to $^7\mathrm{Li} + p$. Because of the difference in the magnetic rigidity of decay products, the identification of the latter is convenient in an electron experiment.

The addition of a proton leads to the excitation of the $\alpha + (hn/tp) + p$ state with $T = 3/2$ (see Fig. 7c), and this could correspond to the isobar analog state ^{9}B(14.655) of width $\Gamma = 0.395$ keV. In studying the coherent dissociation of ^{10}C nuclei at an energy of 2 GeV per nucleon, it was found that the 2He2H channel is leading (82%), which is due largely to ^{9}B decays (30%) (for an overview, see [5]). Perfect agreement of the ground-state decays $^9\mathrm{B} \to {}^8\mathrm{Be}$ manifested itself, which renders ^{10}C an efficient source of ^{9}B. Available angular measurements in $^{10}\mathrm{C} \to 2\alpha 2p$ white stars make it possible to verify the presence of

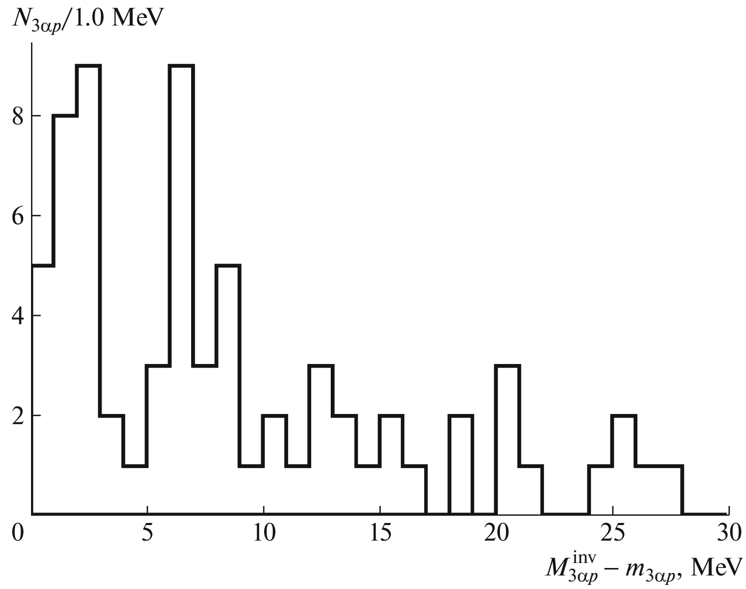

Fig. 8. Distributions of the invariant mass $Q_{3\alpha p}$ in 60 ^{14}N $\to 3\alpha p$ events.

^{9}B(14.655) decays in them. They are supplemented with measurements for $2\alpha 2p$ stars containing target fragments or product mesons, the statistics of these measurements being improved.

To date, searches for ^{14}N $\to 3\alpha(+\text{H})$ events at an energy of 2 GeV per nucleon have been quickened on the basis of transverse scanning of NTE layers. The leading role of the 3HeH channel in the distribution of the fragmentation channels preserving the charge of ^{14}N was revealed, and the contribution of the decay process ^{8}Be $\to 2\alpha$ was estimated at 25% to 30% [6, 17]. The initial goal was to determine the ^{8}Be, ^{9}B, and Hoyle state contributions. Since ^{14}N fragmentation turns out to be a source of $3\alpha p$ ensembles, the isobar analog state ^{13}N(15.065) of isospin $T = 3/2$ in the excitation spectrum of ^{13}N at 5.6 MeV above the ^{9}Bα threshold becomes yet another object of investigations. Because of forbiddenness in isospin, the width of ^{13}N(15.065) is as small as $\Gamma = 0.86$ keV. In principle, ^{12}C$(0^+_2)p$ and ^{9}Bα decays, each having a probability of 5%, may be signatures of ^{13}N(15.065) [18].

Let us consider the ^{13}N(15.065) state within the α-cluster scenario in Fig. 7*d*. The values of $T = 3/2$ and $J = 3/2$ are possible in the $2\alpha + (hn) + p$ and $2\alpha + (tp) + p$ configurations involving hn or tp virtual pairs of spin $J = 1$. The transition is possible via S-wave nucleon spin flip in the $3\alpha p$ ensemble without completely overcoming the hn and tp binding threshold (about 20 MeV). The decay of ^{13}N(15.065) is initiated by the return of the nucleon to the alpha-particle cluster, the released energy being spent to proton emission or alpha-particle emission, and the excited and ground states of ^{12}C and ^{9}B nuclei, respectively. As a signal of the branch of isobar analog states, the discovery of the decay ^{14}N $\to ^{13}$N(15.065) would be a motivation to perform their searches in the fragmentation of neighboring nuclei. Searches for the $T = 1$ ^{14}N(>20.4 MeV) state by its decays to $3\alpha d$, which are also suppressed in isospin, are yet another possibility.

Figure 8 illustrates the status of the analysis. It shows evidence of the possible presence of an isobar analog state in the range between 5 and 9 MeV above the $3\alpha p$ threshold, and this is satisfactory within the approach used. Thus, a bound alpha particle manifests itself as an elastically deformable object that forms a basis of the whole family of quite long-lived states. Its relaxation to an S-wave state determines final states of the decays of isobar analog states.

6. CONCLUSIONS

The status of the BECQUEREL experiment aimed at studying hotly debated problems of nuclear-cluster physics is presented. Owing to a unique sensitivity and a high spatial resolution, the NTE method used permits studying, within a unified approach, multiparticle final states arising upon the dissociation of a wide variety of nuclei.

Investigations performed at the present time focus on the concept of alpha-particle Bose–Einstein condensate of an ultracold state of several S-wave alpha particles near binding thresholds. The unstable nucleus ^{8}Be is described as a 2αBEC state, while the ^{12}C(0^+_2) excitation or the Hoyle state is described as 3αBEC. The decays ^{8}Be $\to 2\alpha$ and

$^{12}C(0_2^+) \to ^8Be\alpha$ may serve as signatures of more complex decays of $n\alpha$BEC. For example, the 0_6^+ state sought in the ^{16}O nucleus at 660 keV above the 4α threshold and treated as 4αBEC may undergo sequential decay through the $^{16}O(0_6^+) \to \alpha^{12}C(0_2^+)$ channel or through the $^{16}O(0_6^+) \to 2^8Be$ channel. Its searches are performed in several experiments thatstudy the fragmentation of light nuclei at low energies. A confirmation of the existence of this and more complex forms of αBEC could provide a basis for extending scenarios of the synthesis of medium-mass and heavy nuclei in nuclear astrophysics.

A treatment of αBEC as an invariant phenomenon suggests the possibility of its searches in NTE layers longitudinally irradiated with relativistic nuclei. In this case, the invariant mass of the ensembles of helium and hydrogen fragments can be determined on the basis of emission angles in the approximation of conservation of the parent-nucleus momentum per nucleon. Owing to extremely low values of the energy and widths, ^{8}Be and Hoyle state decays, as well as the decay process $^9B \to ^8Bep$, are readily identifiable in the fragmentation of light nuclei upon setting an upper cut on the invariant mass.

Once having been tested, this approach came to be applied in identifying ^{8}Be and the Hoyle state and in searching for more complex $n\alpha$BEC states in the fragmentation of medium-mass and heavy nuclei. On the basis of a statistical data sample including several tens of ^{8}Be decay events, it has recently been found that the probability for observing ^{8}Be in an event grows with increasing number of relativistic alpha particles in it. A preliminary conclusion that the contributions of ^{9}B and Hoyle state decays also grow was drawn. Exotically large dimensions and long lifetimes of the ^{8}Be nucleus and Hoyle state give grounds to assume the possibility of synthesis of αBEC via the sequential alpha-particle fusion $2\alpha \to ^8Be$, $^8Be\alpha \to ^{12}C(0_2^+)$, $^{12}C(0_2^+)\alpha \to ^{16}O(0_6^+)$, $2^8Be \to ^{16}O(0_6^+)$ and so on, with a probability decreasing at each step, upon the emission of photons or recoiling particles.

The main task of the forthcoming stage is to clarify the connection between the emergence of the ^{8}Be nucleus and Hoyle state, on one hand, and the multiplicity of alpha-particle ensembles, on the other hand, and to perform, on this basis, searches for decays of the $^{16}O(0_6^+)$ state. In this connection, the BECQUEREL experiment is aimed at measuring multiparticle channels of fragmentation of ^{84}Kr nuclei at energies of up to 1 GeV per nucleon. The available number of NTE layers is sufficient for reaching the required level of statistics via transverse scanning of these layers. The data presented in this article is the first contribution to the object-oriented search for 4αBEC. Although the data that we obtained are promising, a confirmation of 4αBEC calls for a severalfold enlargement of statistics.

As a continuation of the studies devoted to the fragmentation of light nuclei, searches for decays of isobar analog states were launched. Manifesting themselves at high excitation energies, but simultaneously having rather small widths, isobar analogous states serve as signatures of the rearrangement of the structure toward similarity to their less stable isobars. An analysis of irradiations of nuclear emulsions with ^{9}Be, ^{14}N, ^{22}Ne, ^{24}Mg, and ^{28}Si nuclei has been revived in this context.

The problems in question can be tackled via the application of the fully motorized Olympus BX63 microscope recently delivered for use in the BECQUEREL experiment. Mastering its potentialities is a particular methodological challenge. We cherish the hope that its application and advances in the analysis of images would give new impetus to the application of the NTE method.

REFERENCES

1. F. Ajzenberg-Selove, Nucl. Phys. A **490**, 1 (1988); TUNL Nuclear Data Evaluation Project.
2. M. Freer and H. O. U. Fynbo, Prog. Part. Nucl. Phys. **78**, 1 (2014). https://doi.org/10.1016/j.ppnp.2014.06.001
3. A. Tohsaki, H. Horiuchi, P. Schuck, and G. Röpke, Rev. Mod. Phys. **89**, 011002 (2017). https://doi.org/10.1103/RevModPhys.89.011002
4. W. von Oertzen, Lect. Notes Phys. **818**, 1 (2010). https://doi.org/10.1007/978-3-642-13899-7_3
5. S. Adachi, Y. Fujikawa, T. Kawabata, H. Akimune, T. Doi, T. Furuno, T. Harada, K. Inaba, S. Ishida, M. Itoh, C. Iwamoto, N. Kobayashi, Y. Maeda, Y. Matsuda, M. Murata, S. Okamoto, et al., Phys. Lett. B **819**, 136411 (2021). https://doi.org/10.1016/j.physletb.2021.136411
6. P. I. Zarubin, Lect. Notes Phys. **875**, 51 (2013). https://doi.org/10.1007/978-3-319-01077-9_3
7. D. A. Artemenkov, V. Bradnova, M. M. Chernyavsky, E. Firu, M. Haiduc, N. K. Kornegrutsa, A. I. Malakhov, E. Mitsova, A. Neagu, N. G. Peresadko, V. V. Rusakova, R. Stanoeva, A. A. Zaitsev, P. I. Zarubin, and I. G. Zarubina, Eur. Phys. J. A **56**, 250 (2020). https://doi.org/10.1140/epja/s10050-020-00252-3
8. B. Borderie, Ad. R. Raduta, G. Ademard, M. F. Rivet, E. de Filippo, E. Geraci, N. Le Neindre, R. Alba, F. Amorini, G. Cardella, M. Chatterjee, D. Guinet, P. Lautesse, E. La Guidara, G. Lanzalone, G. Lanzano, et al., Phys. Lett. B **755**, 475 (2016). https://doi.org/10.1016/j.physletb.2016.02.061

9. M. Barbui, K. Hagel, J. Gauthier, S. Wuenschel, R. Wada, V. Z. Goldberg, R. T. deSouza, S. Hudan, D. Fang, X.-G. Cao, and J. B. Natowitz, Phys. Rev. C **98**, 044601 (2018). https://doi.org/10.1103/PhysRevC.98.044601
10. R. J. Charity, K. W. Brown, J. Elson, W. Reviol, L. G. Sobotka, W. W. Buhro, Z. Chajecki, W. G. Lynch, J. Manfredi, R. Shane, R. H. Showalter, M. B. Tsang, D. Weisshaar, J. Winkelbauer, S. Bedoor, D. G. McNeel, et al., Phys. Rev. C **99**, 044304 (2019). https://doi.org/10.1103/PhysRevC.99.044304
11. J. Bishop et al., Phys. Rev. C **100**, 034320 (2019). https://doi.org/10.1103/PhysRevC.100.034320
12. R. Smith, J. Bishop, J. Hirst, Tz. Kokalova, and C. Wheldon, Few Body Syst. **61**, 14 (2020). https://doi.org/10.1007/s00601-020-1545-5
13. S. Manna, T. K. Rana, C. Bhattacharya, S. Kundu, R. Pandey, K. Banerjee, Pratap Roy, A. Sen, T. K. Ghosh, G. Mukherjee, Debasish Mondal, Md. Moin Shaikh, J. K. Meena, P. Karmakar, D. Paul, K. Atreya, et al., Eur. Phys. J. A **57**, 286 (2021). https://doi.org/10.1140/epja/s10050-021-00592-8
14. A. A. Zaitsev, D. A. Artemenkov, V. V. Glagolev, M. M. Chernyavsky, N. G. Peresadko, V. V. Rusakova, and P. I. Zarubin, Phys. Lett. B **820**, 136460 (2021). https://doi.org/10.1016/j.physletb.2021.136460
15. S. A. Krasnov, T. N. Maksimkina, G. J. Musulmanbekov, F. Schussler, A. Dirner, L. Just, M. Karabová, A. Pavuková, M. Tóthová, S. Vokál, J. Vrláková, B. Jakobsson, K. Soderstrom, M. I. Adamovich, M. M. Chernyavsky, S. P. Kharlamov, et al., Czech J. Phys. **46**, 531 (1996). https://doi.org/10.1007/BF01690674
16. J. F. Ziegler, J. P. Biersack, and M. D. Ziegler, Nucl Instrum. Methods Phys. Res., Sect. B **268**, 1818 (2010). https://doi.org/10.1016/j.nimb.2010.02.091
17. T. V. Schedrina, V. Bradnova, M. M. Chernyavsky, S. P. Kharlamov, A. D. Kovalenko, M. Haiduc, A. I. Malakhov, G. I. Orlova, P. A. Rukoyatkin, V. V. Rusakova, S. Vokal, A. Vokalova, P. I. Zarubin, and I. G. Zarubina, Phys. At. Nucl. **70**, 1230 (2007); nucl-ex/0605022. https://doi.org/10.1134/S1063778807070149
18. E. G. Adelberger, A. B. McDonald, C. L. Cocke, C. N. Davids, A. P. Shukla, H. B. Mak, and D. Ashery, Phys. Rev. C **7**, 889 (1973). https://doi.org/10.1103/PhysRevC.7.889